Available online at www.sciencedirect.com
SCIENCE DIRECT
European Journal of Medicinal Chemistry 41 (2006) 795–808
EUROPEAN JOURNAL OF MEDICINAL CHEMISTRY
http://france.elsevier.com/direct/ejmech

Invited review

Computational approaches for predicting CYP-related metabolism properties in the screening of new drugs

P. Crivori, I. Poggesi *

Prediction and Modeling, Nerviano Medical Sciences S.r.l., Nerviano Medical Sciences S.r.l., Viale Pasteur 10, 20014 Nerviano (MI), Italy

Received 6 September 2005; received in revised form 9 March 2006; accepted 16 March 2006
Available online 27 April 2006

Abstract

The site of biotransformation, the extent and rate of metabolism and the number of active metabolic pathways are among the most important characteristics of the pharmacokinetics of a drug. The catalytic activity of drug metabolizing enzymes is likely the most influential determinant of the pharmacokinetic variability. Metabolic stability is the prerequisite for sustaining the therapeutically relevant concentrations. Metabolic inhibition and induction can give rise to clinically important drug–drug interactions. A variety of computational approaches are currently available for predicting different cytochrome P450 (CYP)-related metabolism endpoints. The present review will describe these approaches and their impact on drug development process. Indications on the available software for the implementation will also be given.

Keywords: CYP regioselectivity; CYP inhibitors; CYP inducers; CYP substrates; Rate of metabolism; Predictive models

1. Introduction

In the last few years the importance of favorable pharmacokinetic characteristics for the development of a successful drug has been widely recognized, so that absorption, distribution, metabolism and elimination (ADME) evaluations are integrated earlier into drug discovery strategies. Following this paradigm, after the introduction of high- or medium-throughput in vitro activity tests, computational tools are becoming more and more popular for screening compounds with regard to the relevant ADME properties [1–5].

Metabolism is one of the most complicated pharmacokinetic properties to be understood and predicted. The metabolic behavior of drugs depends not only on the physicochemical properties of compounds, but also on the characteristics of the involved metabolizing system, whose expression depends in turn on a number of genetic and environmental factors. The site(s) of biotransformation (i.e. regioselectivity), substrate selectivity, extent and rate of metabolism, inhibition and induction properties are the most important aspects of the metabolic behavior of new compounds. Their relevance is easily understood in the process of drug discovery and development. It may be difficult to sustain the therapeutically relevant concentrations of rapidly metabolized compounds. Metabolic inhibition, induction and/or competition for the same metabolic pathways can give rise to clinically important drug–drug interactions. In principle, metabolism is important for the elimination of drugs from the body and the subsequent inactivation, but it also can lead to the formation of pharmacologically active or toxic metabolites. All these aspects should be evaluated as early as possible during the drug discovery process. In this respect, computational tools can be used either for avoiding potential metabolic issues or as alerts for including in the development program appropriate evaluations of their relevance. Since cytochromes P450 (CYPs) are the most important phase I enzyme systems involved in drug metabolism [6], pharmaceutical companies mainly focus their attention on evaluating CYP-related endpoints for potential drug candidates [7]. Huge amounts of in vitro metabolic stability as well as inhibition data obtained with recombinant CYP preparations or liver preparations (microsomes, hepatocytes, slices, etc.), have been generated. During the past several years a substantial progress in understanding

* Corresponding author. Present address: GlaxoSmithKline, Clinical pharmacokinetics, Via Fleming, 2, 37135 Verona, Italy.
E-mail address: italo.2.poggesi@gsk.com (I. Poggesi).

0223-5234/$ - see front matter © 2006 Elsevier SAS. All rights reserved.
doi:10.1016/j.ejmech.2006.03.003

CYP structure and mechanism has also been gained based on the three-dimensional (3D) structures of bacterial enzymes [8]. Although these share only low sequences homology with mammalian enzymes, certain regions of primary interest, such as the heme and oxygen binding sites, are quite conserved among different species. A substantial increase in this knowledge will derive from the solution of the mammalian CYP structures using X-ray crystallography. Until recently, this approach was thought to be impossible due to considerable difficulties in obtaining crystals; however, the first papers on a rabbit (CYP2C5) and two human CYP isoforms (CYP2C9 and CYP3A4), both unliganded and in complex with few substrates and inhibitors, appeared recently in the literature (Fig. 1) [9–13]. The increasing knowledge of CYP structure, activity and regulation, together with the generation of new data, is giving momentum to the development of computational models intended to predict the metabolic endpoints of new compounds. In a recent comprehensive review on the modeling approaches on CYPs activity and substrate selectivity the methodologies were classified as ligand, protein or ligand–protein interaction-based approaches [14]. Ligand-based approaches are modeling methods that use the structural information of the molecules interacting with the target (i.e. CYP(s)) of interest. These approaches include quantum mechanics (QM) methods, quantitative structure–activity/property relationships (QSAR or QSPR), three-dimensional QSAR (3D-QSAR) and pharmacophore generation. QM methods are based on ab initio or semi-empirical calculations for providing a description of the electronic structure of ligands and for calculating the activation energies of a given reaction. QSAR are mathematical relationships linking chemical structure (encoded by calculated descriptors) and metabolic properties in a quantitative manner. Various linear and non-linear statistical techniques in combination with different molecular descriptors can be used for such purpose. 3D-QSAR involves the analysis of the quantitative relationship between the biological activity of a set of aligned compounds and their 3D electronic, steric and hydrophobic properties. Pharmacophore generation is a procedure to identify, from a series of molecules characterized by a similar metabolic property, the common structural features and their 3D spatial arrangements assumed to be responsible for that activity. Protein-based methods rely upon the structural information extracted from the X-ray crystallographic and/or homology protein structures. These also include docking techniques for the exploration of possible binding modes of a ligand to a given enzyme or receptor. In the ligand–protein interaction-based (mixed) approaches, a synthesis of the information on both ligands and proteins is attempted, in relationship to the relevant metabolic property.

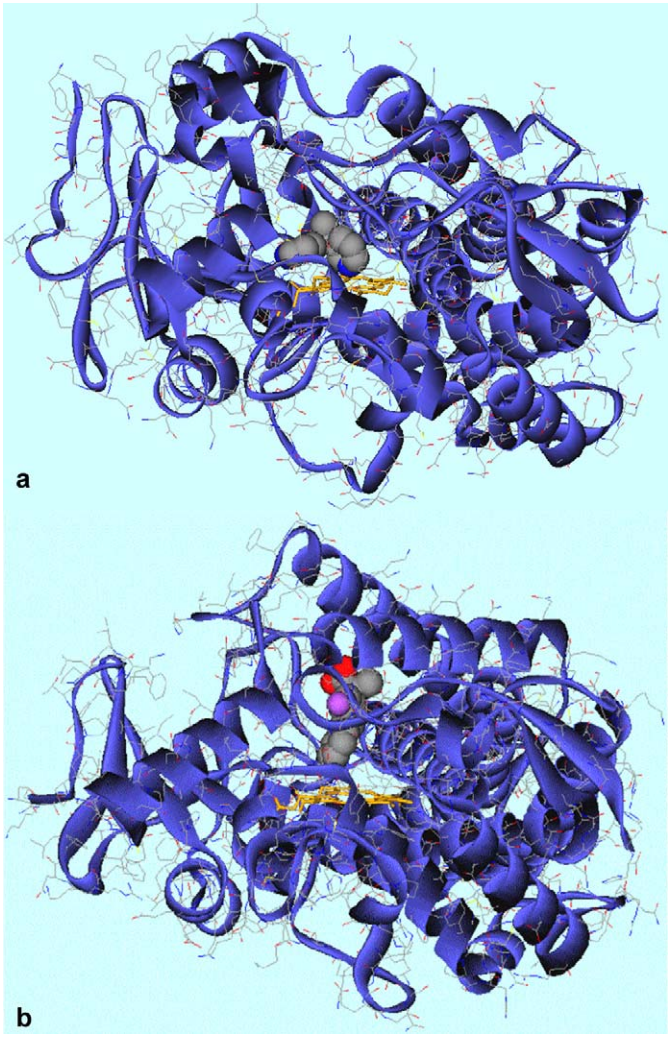

Fig. 1. X-ray crystallographic structures of human CYPs a) CYP3A4 in complex with metyrapone inhibitor (1WOG Protein Data Bank code), b) CYP2C9 in complex with flurbiprofen substrate (1R9O Protein Data Bank code).

In this review, the classification mentioned above will be used; however, since the attempt is to describe approaches related to more general CYP-mediated properties of drug candidates, the text will be mainly structured by metabolism endpoint. Depending on the data and structural information used, these models can have local or more general applicability in metabolism predictions.

2. Prediction of regioselectivity

The prediction of the most likely metabolic labile site(s) of a drug candidate can be relevant for several reasons. For example, once the labile sites have been identified, lead compounds can be optimized adopting the appropriate structural modifications aiming to reduce the rate of metabolism and/or avoid the formation of potential toxic metabolites. For example, the major metabolic pathway of tolbutamide is the oxidation by CYP2C9 of the benzylic methyl group. This pathway is inactive in chlorpropamide, which incorporates a chlorine atom in this position. This modification reduces the plasma clearance and increases the half-life (approximately from 5 to 35 h) and, in turn, the duration of action [15]. In silico prediction of the potential labile sites could also provide assistance for the identification of the chemical structures of metabolites experimentally determined by mass spectroscopy techniques [16]. A summary of the reviewed approaches is reported in Table 1.

Table 1
Computational approaches for modeling CYP regioselectivity

Endpoint	Training set	Experimental data	Methodology	References
Ligand-based approaches				
CYP-mediated aliphatic oxidation	Organics	Sites of biotransformation	Semi-empirical QM calculation	[17,18]
CYP-mediated aromatic oxidation	Organics	Sites of biotransformation	Semi-empirical QM calculations	[19]
CYP3A4-mediated hot spots	Drugs	Sites of biotransformation	Trend vector model	[20]
Protein-based approaches				
CYP regioselectivity	Drugs	Sites of biotransformation	Docking of substrates into CYP homology models	[21–30]
Mixed approaches				
CYP2D6 mediated hydroxylation and O-dealkylation	Drugs	Sites of biotransformation	Docking into CYP2D6 homology model, pharmacophore and MO calculations	[31]
CYP2D6 mediated N-dealkylation	Drugs	Sites of biotransformation	Docking into CYP2D6 homology model, pharmacophore and MO calculations	[32]
CYP2C9 mediated oxidation	Drugs	Sites of biotransformation	Docking into CYP2C9 homology model, pharmacophore and MO calculations	[33]
CYP2C9 mediated hydrogen abstraction	Drugs	Sites of biotransfomation	GRID-based characterization of homology enzyme binding site and substrates followed by similarity analysis	[34]

2.1. Ligand-based approach

Based on the assumption that the ability of a compound to be metabolized by a particular CYP isoenzyme mainly depends on its physicochemical characteristics, some authors developed models for predicting the site(s) of biotransformation based on the structural features of the molecules, without taking into account the enzyme active site. These methods mainly rely upon QM approaches for calculating the energies involved in the process.

Korzekwa et al. [17,18] applied semi-empirical QM methods for predicting the regioselectivity of CYP-mediated hydrogen atom abstraction reactions. This approach was based on the assumption that the relative tendency of hydrogen atom abstraction by the CYP enzymes was due to the stability of the formed radical. The developed electronic model was able to predict aliphatic hydroxylation, amine dealkylation, and O-dealkylation of relatively small and hydrophobic molecules for which the substrate–protein interactions would have only a marginal effect on regioselectivity. More recently, the predictive capacity of such model was extended to CYP-mediated aromatic hydroxylation [19]. This computational model combined experimental data and semi-empirical QM calculations to predict the activation energies for aromatic and aliphatic hydroxylation of relatively small molecules. The model was expected to work better with substrates and enzymes that showed little preference in their active site orientation upon binding, such as CYP1A2, CYP2B1, CYP2B4, CYP2E1 and CYP3A4. For larger compounds with an increased number of functional groups, electronic models should be combined with approaches that also accounts for the binding effects.

Singh et al. [20] developed a rapid semi-quantitative model for identifying CYP3A4-mediated "hot spots". The model was based on the assumption that the CYP3A4 substrate liability was mainly dependent on the electronic environment surrounding the hydrogen atoms. In addition, it was assumed that the extraction of a hydrogen atom was the rate-determining step. Therefore, the model was based on the energy needed to remove a hydrogen radical from each molecular site and the surface area exposure of the hydrogen atom. Since AM1 semi-empirical QM calculations were too time consuming for routine work, the authors developed a statistical trend vector model to estimate the AM1 abstraction energy of a hydrogen atom from its local atomic topological environment. With this model the hydrogen abstraction energies of 50 CYP3A4 substrates, not included in the original model, were predicted. It was found that 78% of the hydrogen atoms with abstraction energy lower than 27 kcal/mol and solvent accessible surface area exposure greater than or equal to 8.0 $Å^2$ were the most susceptible ones for CYP3A4-mediated hydroxylation. The approach was rapid and accurate, even if in few cases it was unable to predict the likely site(s) of metabolism.

2.2. Protein-based approaches

Since the metabolically labile positions within a substrate should be in close proximity to the reactive center of the CYP metabolizing enzyme (i.e. the heme), many authors were able to correctly identify the sites of metabolism by studying the substrate–enzyme complexes. Historically, several protein-based approaches relied on crystal structure information obtained from bacterial homologues. These models were mainly used to analyze specific substrate–enzyme interactions in an attempt to rationalize observed metabolic transformation. Therefore, several authors [21–30] docked a set of known substrates into the active sites of corresponding CYP enzymes. In general, the docking results obtained were consistent with experimental site-direct mutagenesis data and metabolite formations, i.e. the oxidative site(s) within a molecule were relatively close and oriented toward the ferric atom of the heme.

2.3. Mixed approaches

In some cases, the information related to the structure of proteins and ligands were combined to provide better predictions of the site of metabolism. In one of these interesting approaches, a homology model, constructed using the bacterial CYP101, CYP102 and CYP108 crystal structures, was used

in combination with a 3D pharmacophore model and QM calculations performed on substrates, metabolic intermediates and products, for predicting CYP2D6-mediated hydroxylation and O-dealkylation of 40 substrates [31]. The combined protein and pharmacophore model was further extended to another pharmacophore to take into account the CYP2D6-mediated N-dealkylation reactions [32]. The resulting model, based on 51 substrates and 72 related metabolic pathways, correctly predicted six of the seven observed CYP2D6-formed metabolites not included in the model and identified two possible metabolites not detected experimentally. The same approach was applied for predicting CYP2C9-mediated metabolism sites of 27 substrates [33]. In this case, the protein homology model was built using the crystal structures of rabbit CYP2C5 and bacterial CYP102. The combined approach correctly predicted the metabolism of four substrates not included in the model. The authors highlighted that this combined methodology increases the understanding of the CYP active sites and their interactions with the substrates, since it takes into account the substrate reactive sites as well as the steric and electronic properties of the surrounding enzyme.

Another combined approach described by Zamora et al. [34] was based on a comparison between alignment-independent descriptors derived from GRID molecular interaction fields (MIF) for the CYP2C9 active site, based on a CYP2C9 homology model developed from rabbit CYP2C5, and a fingerprint-distance representation of all hydrogen atoms present in a potential substrate. The Carbó similarity index was used to compare the CYP2C9 active site with all the hydrogen atoms present in the substrates. The different hydrogen atoms present in any substrates were ranked according to the total similarity index. Hydrogen atoms with the highest similarity represented the most likely sites to undergo oxidative metabolic reactions. The method was validated with 87 CYP2C9-catalyzed oxidative reactions reported in the literature for 43 different substrates. In more than 90% of these cases, the hydrogen atom ranked at the first, second or third position was the experimentally reported site of oxidation.

In general, in the approaches to the prediction of the site of metabolism it is difficult to define consistent endpoints for comparison of different methodologies. In certain cases it may be important to identify the individual, most important biotransformation pathway. In case of metabolism-mediated toxicity, on the contrary, it may be more important to predict minor pathways. In any case, the mixed approaches, making use of the information gained from both ligand and protein structure, are likely the most efficient approach to the problem.

3. Prediction of CYP substrate specificity

Although all approaches reported above are useful to identify the most likely sites of CYP-mediated metabolism for compounds, none of them are able to predict whether a molecule will be a substrate, non-substrate or inhibitor of a particular CYP isoform. In this respect, QSARs, alone or in combination with protein structure-based homology models, have been applied for predicting CYP substrate specificity. A summary of the models described below are reported in Table 2. In general, lead candidates that are a substrate of a specific CYP isoform (for example, CYP2D6) tend to be deprioritized in drug discovery, due to the difficulties (e.g. polymorphism, drug–drug interactions) that will be encountered in the subsequent development [35].

3.1. Ligand-based approaches

Many approaches have been proposed for identifying substrates of the different CYPs based on the common structural features of series of compounds known to be metabolized by a specific isoenzyme.

Table 2
Computational tools for modeling CYP substrate specificity

Endpoint	Training set	Experimental data	Approach	References
Ligand-based approaches				
CYP3A4 substrates	38 drugs	K_m	Catalyst pharmacophore and PLS-QSAR	[36]
CYP2B6 substrates	16 drugs	K_m	Catalyst pharmacophore and PLS-QSAR	[37]
CYP1A2, 2A6, 2B6, 2C9, 2C19, 2D6, 2E1 and 3A4 substrates	11, 6, 10, 8, 8, 10, 10, 10 drugs, respectively	K_d and K_m	MLR-QSAR using logP, $logD_{7.4}$, H-bond donors, acceptors, LUMO and HOMO energies, ionization potential and dipole moments.	[38]
CYP2D6 substrates	24 drugs	K_m	CoMFA model	[39]
CYP substrates and non-substrates	485 substrates and 523 products	Substrates and products for 38 CYPs	Kohonen learning approach applied to calculated descriptors (size, H-bonding potential, charge, lipophilicity, reactivity)	[40]
CYP3A4 substrates and inhibitors	491 drug-like	K_m	Kohonen learning approach applied to calculated descriptors (lipophilicity, H-bonding potential, flexibility)	[41]
Ligand and protein mixed approaches				
CYP2B6 substrates	16 drugs	K_m	Catalyst pharmacophores and CYP2B6 homology modeling	[42]
CYP1A2, 2D6 and 3A4 substrates	50 drugs	CYP1A2, 2D6 and 3A4 substrates and non-substrates	Semi-quantitative models based on calculated characteristics of substrates (LUMO, volume and surfaces) and substrate-CYP homology model complexes	[43]
CYP2D6 substrates	24 drugs	K_m	CoMFA model and CYP2D6 homology model	[44]

The $K_{m(apparent)}$ data of 38 known CYP3A4 substrates taken from different literature sources were used to build a pharmacophore model using the Catalyst software [36]. The pharmacophore consisted of four features: two hydrogen bond acceptors, one hydrogen bond donor and one hydrophobic region. The distance of the two inter-hydrogen bond acceptor was 7.7 Å, whereas the hydrophobic region and hydrogen bond donor were 6.6 and 6.4 Å away from one of the hydrogen bond acceptors, respectively (Fig. 2). The model was able to predict all $K_{m(apparent)}$ values of 12 substrates in the test set with residuals smaller than 1 log unit. A similar approach was used for CYP2B6 [37]. Two different QSAR analyses were developed on a small training set of 16 substrates using $K_{m(apparent)}$ values generated with B-lymphoblastoid expressed CYP2B6. A pharmacophore model generating from Catalyst was compared with a partial least squares (PLS) model developed using surface-weighted holistic invariant molecular (MS-WHIM) descriptors. This pharmacophore hypothesis produced four important features for ligand binding to the active site, namely three hydrophobes and one hydrogen bond acceptor. The three hydrophobic regions present in the pharmacophore were located at distances of 5.3, 3.1, and 4.6 Å from the hydrogen bond acceptor, and had intermediate angles of 72.8 and 67.6°. The leave-one-out cross-validation of PLS gave a good q^2 value of 0.607. The pharmacophore and PLS MS-WHIM models were then validated with an external set of five compounds covering a narrow range of $K_{m(apparent)}$. Both models failed to predict one compound in the test set, while for the remaining four the predictions showed error less than 1 log unit.

A set of quantitative structures metabolism relationships for identifying CYP1A2, CYP2A6, CYP2B6, CYP2C9, CYP2C19, CYP2D6, CYP2E1 and CYP3A4 substrates has been published by Lewis et al. [38]. The K_d and K_m values, expressed as RT$logK_d$ or RT$logK_m$, were correlated by multiple linear regression (MLR) analysis with descriptors related to lipophilicity, polarity and electronic molecular properties. Such descriptors included logP, $logD_{7.4,}$ number of H-bond donors and acceptors, the lowest unoccupied molecular orbital (LUMO) and the highest occupied molecular orbital (HOMO) energies, ionization potential and dipole moments. Although the models are easily interpretable, they have limited value since they were based on a few data and were not evaluated with external data sets.

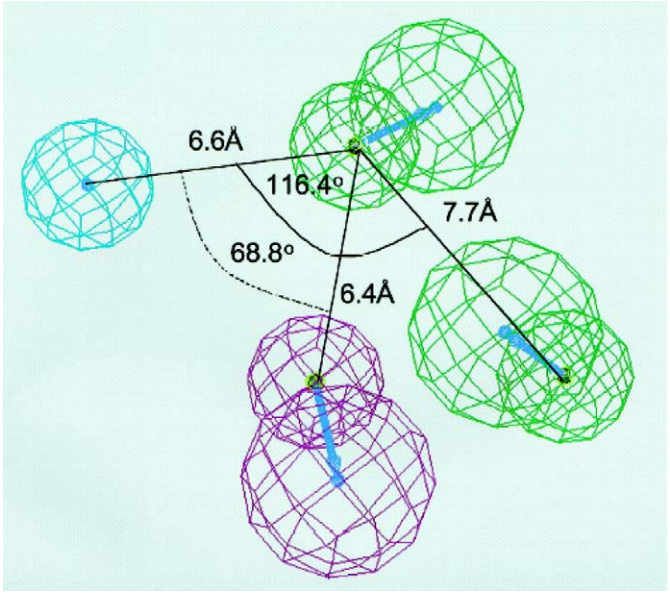

Fig. 2. Pharmacophore features and spatial arrangements of CYP3A4 substrates. Color code: hydrophobic areas: cyano, hydrogen bond donor features: purple, hydrogen bond acceptor features: green. Vectors show the direction of the putative hydrogen bond donors (from Ref. [36]).

Haji-Momenian et al. [39] applied a comparative molecular field analysis (CoMFA) to predict the substrate specificity towards CYP2D6 enzyme. The model was based on a training set of 24 substrates with experimental K_m values from liver microsomal CYP2D6 spanning more than 3 log units. The CoMFA model obtained was tested predicting the K_m values of 15 substrates which are not present in the training set. A correlation coefficient r^2 for the predicted versus observed K_m values of 0.62, demonstrated the predictive ability of the model described.

Using an unsupervised machine learning approach, structure metabolism relationships were developed to discriminate between human CYP substrates and non-substrates [40]. The study involved several steps including a collection of 2200 substrates-products for 38 human CYPs. After determination of the most typical CYP-mediated metabolic reactions for each group, a set of 485 CYP substrates and 523 products were analyzed using unsupervised Kohonen learning approach and a set of seven selected descriptors related to molecular size, H-bonding potential, surface charge properties, lipophilicity and reactivity. Substrates and products occupied distinct areas on the generated Kohonen self-organizing maps (SOMs). The model was able to correctly classify 76.7% of substrates and 62.7% of products, as defined by their localization in the corresponding area of the Kohonen maps. SOMs were also developed for each group of CYP1A1, 1A2, 2C19, 2C9, 2D6, 2E1, and 3A4 specific substrate selected. The substrates for CYP2C9 and CYP2E1 were widely distributed within the map, while substrates for the remaining isoenzymes were mapped in different distinct areas. The model was not validated with any external set of data, but, in theory, it could be used to predict the CYP specificity of potential substrates.

SOMs were also developed to discriminate compounds with low (< 10 μM) or high K_m (> 100 μM) values [41]. In this study a set of 491 drug-like compounds with experimentally apparent K_m values versus 12 human CYPs, was used. After calculating six molecular descriptors related to molecular lipophilicity, H-bonding potential and molecular flexibility, unsupervised learning classification models were developed for each CYP and the entire K_m data set. Only the SOM for CYP3A4 was statistically significant, able to correctly classify 91% high K_m and 97% low K_m molecules. Since compounds that bind human CYP may also act as inhibitors, two sets of 33 and 15 CYP3A4 competitive inhibitors, respectively, were processed on the CYP3A4 SOM. Ninety-four percent and 87% of the two data sets were located in the areas of low K_m CYP3A4

molecules. The non-linear SOM developed was proposed as a high-throughput filter for early identification of potential CYP3A4 substrates/inhibitors.

3.2. Mixed approaches

In some of the approaches, the characteristics of the ligands were combined with the information on the protein structure to obtain predictive models for evaluating substrate specificity. Wang and Halpert [42] published a combined pharmacophore and homology model for CYP2B6 substrates. The training and test sets used in this study were similar to those used in one of the above reported papers [37]. A 3D model of CYP2B6 was built based on the crystal structure of CYP2C5. The reaction metabolic sites present in all 16 CYP2B6 substrates used as the training set were aligned and two Catalyst pharmacophores models generated. Both pharmacophores, which include two hydrophobic regions and one hydrogen bond acceptor, were found to be complementary but located in two different regions of CYP2B6 homology model. Combining the CYP2B6 structural information with the two pharmacophores, the $K_{m(apparent)}$ values of four out of five compounds not included in the training set, were predicted with an error less than 0.7 log unit.

Semi-quantitative models for predicting the substrate specificity towards CYP1A2, CYP2D6 and CYP3A4 enzymes were obtained by analyzing the CYP active sites and a set of specific and non-specific substrates unbound and bound with the three CYP enzymes [43]. The 3D models of CYP1A2, CYP2D6 and CYP3A4 were built using the X-ray crystallography structures of four bacterial cytochromes as templates. It was highlighted that some of the structural differences among 1A2, 2D6 and 3A4 resided in the shape and dimensions of the binding sites. For example, the cavities of CYP1A2 (almost flat according to the structural features of its substrates) and 2D6 were smaller than that of 3A4. Fifty compounds, including specific and non-specific CYP substrates, were docked in the cytochromes using the program DOCK. The total interaction energies (IE_{tot}) and the van der Waals contribution to the total interaction energies (IE_{vdw}) of the substrate–enzyme minimized complexes, were found important descriptors for predicting CYP substrate specificity. For example, the binding of substrate into the 2D6 active site should be mainly favored by hydrogen bonding and electrostatic interactions. In contrast, van der Waals attractive interactions mainly stabilized the complexes involving the enzymes 1A2 and 3A4. In addition, descriptors calculated from the unbound substrates such as the energy of LUMO (E_{LUMO}), molecular volume (V_{mol}) and the ratio between the hydrophilic component and the total solvent accessible surface (S_{phi}/S_{tot}), were found relevant for substrate specificity. Based on these analyses, an interesting protocol summarized below was proposed for predicting the specificity of a substrate towards 1A2, 2D6 and 3A4 enzymes:

- A substrate, to be specific for 2D6, should carry a protonated nitrogen atom and have van der Waals contribution to the total interaction energies for its complex with 2D6, expressed as a ratio between IE_{vdw} and IE_{tot} (IE_{vdw}/IE_{tot}), significantly lower than 0.8. For the same compounds, IE_{vdw}/IE_{tot} for the substrate-1A2 and 3A4 complexes should have values close or lower than 0.83.
- Specific substrates for 1A2 and 3A4 may be neutral or protonated. 2A) Protonated substrates specifically for either 1A2 or 3A4 should display IE_{vdw}/IE_{tot} values for their complexes with each of the three cytochromes close to or higher than 0.83. Since IE_{vdw}/IE_{tot} is not able to discriminate 1A2 from 3A4 specific substrates, other parameters such as IE_{tot}, V_{mol} should be taken into account. The following rules should work also for neutral substrates. 2B) A neutral or protonated substrate may be predicted specific for 1A2 when V_{mol} is lower than 200 Å^3 and IE_{tot} of its complexes with 1A2 and 3A4 is higher than –40 kcal/mol. On the other hand, a specific substrate for 3A4 should have a V_{mol} greater than 275 Å^3 and an IE_{tot} of its complexes with 1A2 and 3A4 significantly lower than –50 kcal/mol. 2C) In addition, size and shape descriptors like V_{mol} and S_{phi}/S_{tot} may be used to improve the predictive power of 1A2/3A4 specificity models.
- Compounds that fail to fulfill the above conditions are predicted to be non-specific substrates.

Using literature K_m values for 24 compounds, a Catalyst pharmacophore model was built to understand the CYP2D6 substrates requirements [44]. This pharmacophore contained one hydrogen bond acceptor, two hydrophobic regions and one positive ionizable feature. It was tested with 28 K_m data not included in the model. An r^2 correlation coefficient of actual versus predicted K_m log transformed values of 0.36 indicated that the model was useful only for ranking external compounds. A 3D model of human CYP2D6 was built based on the crystal structure of mammalian CYP2C5. Docking studies on fluoxetine attempted to rationalize its metabolite formations. The pharmacophore was superimposed onto the docked fluoxetine and it represented the active site of CYP2D6 reasonably well with the exception of the hydrogen acceptor feature.

4. Prediction of rate and extent of metabolism

The drug discovery programs in many pharma industries include assays for screening out the compounds characterized by low metabolic stability. However, only few examples of models for predicting the rate and, in turn, extent of metabolism can be found in the literature (Table 3). In most cases only ligand-based approaches are available, despite the complexity of this multifactorial property. The absence of comprehensive approaches that take into consideration for instance both protein and ligand structures, the activation energies and the exit rate of the biotransformation products is the likely reason why the development of predictive models for estimating the metabolization rate is probably lagging behind in comparison to some of the other CYP-related properties.

Table 3
Computational tools for modeling rate and extent of metabolism

Endpoint	Training set	Experimental data	Approach	References
Human intrinsic clearance	26 and 18 drugs	CLint	Catalyst pharmacophore and QSAR	[45]
Human metabolic stability	631	Categories based on % stability in human S9	K-nearest neighbor QSAR (topological descriptors)	[46]
Rat metabolic stability	87 calcitriol analogs	Percent stability in rat S9	PLS-QSAR (BCUT, Qikprop, topological descriptors)	[47]
Human CYP3A4 metabolic stability	1800	Categories based on % stability in human CYP3A4	PLSD-QSAR (Volsurf, GRIND descriptors)	[48]
In vitro CYP3A4 and CYP2D6 N-dealkylation rate	83	V_{max}	NN-QSAR (geometry, electronic and H-bond potentials descriptors)	[49]

An attempt to predict in vitro human intrinsic clearance (CLint) was done by using Catalyst-based pharmacophore and descriptor-based QSAR analyses [45]. Two training sets, consisting of 26 and 18 molecules, were modeled separately. The 26 ligand-based pharmacophore consisted of two hydrophobes, a hydrogen bond acceptor and an aromatic ring feature, while the 18 compound-based model contained two hydrogen bond acceptors, a hydrophobe, and a positive ionizable feature. Although the two sets generated markedly different phamarcophores, each of these models was used to predict the CLint in the other data set. As expected, poor predictive power characterized both models. An alternative technique was applied for modeling the previous data sets. Two different descriptor-based QSAR equations were generated but none of them showed an improved predictive performance compared to the pharmacophore models.

Descriptor-based QSPR models were applied for modeling the metabolic turnover rate measured in human S9 homogenates of 631 compounds [46]. The analyzed molecules were divided in four classes (i.e. stable, moderately stable, moderately unstable, unstable) according to their experimental percent turnover. The models were developed with topological molecular descriptors such as molecular connectivity indices or atom pairs using the k-nearest neighbor variable selection optimization method. About 90% of the whole data set was used to develop the models while the remaining 10% being used to test. The models were additionally validated with a set of ~100 compounds including ~65% of stable molecules. The average accuracy of all models in assigning external compounds to the stable class was 85%. Although the models appeared reasonably good in predicting stable compounds, they cannot be easily reproduced since structural information and model parameterizations were not disclosed.

QSAR models were developed to predict the metabolic stability of calcitriol analogs [47]. A set of 130 analogs with known values of in vitro metabolic stability determined in rat post-mitochondrial liver fraction (S9), was used to develop the models. A total of 201 descriptors, including 161 standard 3D BCUT, 31 physicochemical properties computed using QikProp software and nine topological indices were calculated for each of the 130 compounds. The metabolic stability data of 87 analogs were correlated to a subset of descriptors selected using five different variable selection methods using PLS. A further PLS model was developed using three of the most commonly selected descriptors in the five different selection methods; i.e. number of double and ether bonds in the side chain attached to carbon 17 and the stereochemistry at carbon 20. The models obtained were tested with an external set of 43 compounds. The QSMR were also applied for predicting the metabolic stability of 244 virtual calcitriol analogs. Twenty of them were then selected and tested for in vitro metabolic stability. The PLS models showed good performance by predicting correctly the metabolic stability of 17 out of 20 selected compounds.

A PLS discriminant (PLSD) model was developed and extensively validated for predicting human CYP3A4 enzyme stability of potential drug candidates [48]. The model was trained using a set of 1800 compounds and validated with two test sets: the first one including 825 compounds from ex-Pharmacia collection and the second one consisting of 20 known drugs. The descriptors, calculated from the 3D MIF (i.e. Volsurf and GRIND descriptors), were correlated to the experimental metabolic stability classes by a PLSD procedure. The model correctly predicted 75% of the first and 85% of the second test set and showed a precision above 86% to correctly select metabolically stable compounds. The PLS coefficients that mostly contribute to explain the PLSD model were also reported, providing indications on how a candidate compound can be modified to improve its stability.

Balakin et al. [49] proposed a neural network (NN) QSPR analysis for modeling N-dealkylation reaction rates mediated by human CYP3A4 and CYP2D6. A total of 83 metabolic N-dealkylation reactions with experimental $\log V_{max}$ values for both enzymes were analyzed in this work. The novelty in this approach resided in using descriptors generated from the whole molecule, the reaction centroid and the leaving group. The final descriptors selected based on different approaches, were then correlated with $\log V_{max}$ values using NN algorithm. The most important whole molecule related descriptors identified encoded geometric, electronic and H-bonding potential properties, whereas the descriptors related to the molecular fragments (i.e. reaction centroid and the leaving group) described mainly the steric hindrance of the reactive centers. The CYP3A4 and CYP2D6 models, characterized by high cross-validated leave-one-out correlation coefficients were validated with external sets of data. A correlation coefficient r^2 of 0.90 and 0.94 between the experimental and predicted V_{max} values for CYP3A4 and CYP2D6 external sets confirmed a good predictive performance of both models.

5. Prediction of inhibitors

Compounds characterized by a strong inhibitory activity of the drug metabolizing enzymes can give rise to even fatal drug–drug interactions. An example of the severity of these events is the rhabdomyolysis caused by the coadministration of statins with CYP inhibitors [50]. The inhibition of CYPs is therefore a liability that discovery programs try to avoid. A variety of approaches (in some cases classified as descriptor-based, protein-based and pharmacophore-based [51]) were used for developing predictive models capable of anticipating the behavior of chemicals toward the inhibition of the most important drug metabolizing enzymes (Table 4).

5.1. Inhibitor-based approaches

Descriptor-based statistical methods are typically proposed as fast filters to be implemented in the first phases of discovery to model inhibition data expressed categorically or quantitatively, in terms of IC_{50}, or inhibition constants (K_i). Recursive partitioning (RP) was proposed for identifying inhibitors of human CYP2D6 [52] on the basis of the published K_i of a set of 100 compounds with diverse structures. Different descriptor families were calculated for all compounds (Cerius2 topological, electrotopological, and physicochemical parameters, fragment keys and 1D similarity scores) and a filtered pool of them was obtained using a Monte Carlo annealing algorithm designed to produce a 25-variable linear least-squares fit of a categorical inhibition variable. Approximately half of the descriptors were 1D similarity indices to specific members of the training set. The approach was able to capture 48/59 (81%) of the inhibitors and 27/41 (66%) of the non-inhibitors, with an overall accuracy of 75%.

RP was also used for the generation of virtual filters for inhibition of CYP2D6 and CYP3A4 [53] by means of Chemtree software. The % inhibition data for the two enzymes (1759 and 1756 compounds, respectively) were used for generating 20 random tree models. These models were applied to an external data set of 98 molecules and they were able to generate a statistically significant rank ordering of the inhibition data (Spearman's $\rho = 0.46$, $P < 0.0001$).

Another virtual screening filter for identifying CYP3A4 inhibition liability [54] was developed using PLS. Different molecular descriptors were used to describe the compounds (among the others those calculated with the CATS software and those proposed by Ghose and Crippen). Inhibition data,

Table 4
Computational approaches for modeling CYP inhibition

Endpoint	Training set	Experimental data	Approach	References
Inhibitor-based approaches				
CYP2D6	100	K_i	RP ensemble approach, 2D descriptors (Cerius2 topological, electrotopological, and physicochemical parameters, fragment keys and 1D similarity scores)	[52]
CYP2D6 CYP3A4	1756	Percent inhibition	RP (Chemtree)	[53]
CYP3A4	311	IC_{50}	PLS or ANN, 1D-2D descriptors (CATS, Ghore and Crippen)	[54]
CYP3A4	(Gentest DB) 290	Categorical	ANN, 2D Unity fingerprints	[55]
CYP1A2	19 Flavonoid derivatives	IC_{50}	MLR/ANN, Hammett constant, HOMO, non-overlap steric volume, partial charge of C3 carbon atom, HOMO π coefficients of C3, C3 and C4 carbon atoms of flavonoids	[56]
CYP2D6	106 inhib/494 non-inhib	Categorical	ANN and Bayesian, Cerius2, E-state keys, Barnard 4096-bit fingerprints, functional class fingerprints, AlogP, molecular weight hydrogen bond donors and acceptors.	[57]
CYP2A5	28	IC_{50}	CoMFA and GOLPE/GRID	[60]
CYP2A5	26 naphthalene, 16 non-naphthalene	IC_{50}	CoMFA	[61]
CYP2A6	28	IC_{50}	CoMFA and GOLPE/GRID	[60]
CYP2A6	26 naphthalene, 16 non-naphthalene	IC_{50}	CoMFA	[61]
CYP3A4	14, 32, 22	K_i, IC_{50}	Catalyst, PLS-WHIM	[63]
CYP2C9	9, 29, 13	K_i, IC_{50}	Catalyst, PLS-WHIM	[64]
CYP2C9	14	K_i	CoMFA	[65,66]
CYP2C9	21 positives, 21 negatives	Categorical	GRIND, PLS-DA	[67]
CYP2C9	21	K_i	GRIND, PLS	[67]
CYP2C9	22	K_i	GRID, PLS	[68]
CYP2D6	6	K_i	CoMFA	[69]
CYP2D6	20, 31	K_i	Catalyst, PLS-WHIM	[70]
CYP2D6	47	K_i	GRIND	[71]
CYP3A4	Approximately 780	IC_{50}	In-house 2D, 2D MOE, Volsurf, VAMP; SVM, PLS-DA	[72]
Protein -based approaches				
CYP2D6	33	K_i	Homology modeling and molecular docking (GOLD)	[73]
Mixed approaches				
CYP2C9	21	K_i	Combined 3D-QSAR (GRID)-homology	[74]

expressed as IC_{50}, were categorized in classes. The PLS model was able to correctly attribute 95% of the molecules of a carefully selected training data set ($N = 311$) and 90% of a semi-independent validation data set of 50 molecules. This approach was reported as better of an artificial neural network (ANN) approach based on the same data.

An ANN model [55] based on the two-dimensional (2D) unity fingerprint descriptors allowed the discrimination between inhibitors and non-inhibitors of CYP3A4. The approach allowed to classify correctly 97% of the inhibitors and 95% of non-inhibitors. The predictions of an external data set of known CYP3A4 inhibitors were correct in eight out of nine cases.

MLR analysis and NN were used for studying the inhibition properties of flavonoid derivatives towards CYP1A2 [56]. A number of descriptors (Hammett constant, the HOMO energy, the non-overlap steric volume, the partial charge of C3 carbon atom, and the HOMO π coefficients of C3, C3 and C4 carbon atoms of flavonoids) were found to play an important role in inhibitory activity.

O'Brien and de Groot [57] used NN and Bayesian approaches to model CYP2D6 inhibition data of 600 compounds (106 positive, 494 negative). NN approaches were applied using Cerius^2, on E-state keys and Barnard 4096-bit fingerprints. The Bayesian-based model was developed in Pipeline pilot using functional class fingerprints, AlogP, molecular weight and count of hydrogen bond donors and acceptors as descriptors. The individual models had an overall accuracy of 80% or above. The adoption of combinations of these models allowed optimizing the identification of the inhibitors (95% correct in one of these combinations, reported as 'recover +ve' model) or providing extremely accurate predictions in a more limited number of cases (99% accuracy in case of the consensus model, which was however applicable to 87% of positives and 75% of negatives). As for a previously described model [52] the conclusion was that the educated use of combination of predictions can provide useful answers. In this respect, the consensus among different approaches is becoming more and more popular for providing more accurate predictions of a variety of ADME and toxicity endpoints [58].

Pharmacophoric methods have also been found useful for identifying the relevant structural features of molecules with respect to metabolism inhibition. To some extent, these approaches are similar to those based on the affinity toward the enzyme proposed for the distinction between substrates and non-substrates, even if, the optimal inhibitor in addition to the tight binding should be a poor substrate [59].

In a series of papers, 3D-QSAR such as CoMFA and GOLPE/GRID methods, were used for investigating the structural properties related to the inhibition of CYP2A5 and 2A6. The approaches were applied to a series of 28 compounds [60] and were further extended to naphthalene derivatives [61]. All models had correlation coefficients after cross-validation (q^2) greater than 0.7. It was recognized that the size of the ring substituent was the major discriminating factor between the 2A5 and 2A6 models. In fact, 2A5 inhibitors were allowed to include larger substituents on the coumarin ring system, while for 2A6 compounds only small substituents lead to more potent inhibitors. In addition, the interpretation of the maps revealed that the most potent 2A6 inhibitors should not include lactone moiety, or maybe any heteroatoms, near the corresponding position. The CoMFA approach was further refined in a more recent publication of the same group, based on the IC_{50} of 26 naphthalene and 16 non-naphthalene derivatives. The ultimate aim of this research was to develop potent and specific CYP2A6 inhibitors that upon coadministration with nicotine will increase its bioavailability in smoking cessation therapy [62]. Presence of negative charge near positions 2, 4, 5 and 7 of the naphthalene ring increased the inhibition potency. On the contrary, negative charge disfavored areas were found near position 8. Also in this case the model was able to predict the inhibition properties of an external set ($N = 6$) of compounds.

Ekins et al. [63] developed different pharmacophore models using Catalyst to evaluate the structural features of competitive inhibitors of CYP3A4. Two different Catalyst pharmacophore models were generated based on the K_i of midazolam 19-hydroxylation ($N = 14$) and cyclosporine A metabolism ($N = 32$). Another Catalyst model was developed based on the IC_{50} of quinine 3-hydroxylation ($N = 22$). The three models included three hydrophobic regions at defined distances and geometries from one or two hydrogen bond acceptor features. The correlation between observed and predicted data for these models ranged from 0.72 to 0.92, with K_i of eight out of nine compounds from an external data set predicted within 1 log unit of observed. On the same data sets, MS-WHIM descriptors were used for developing PLS QSAR models. The models showed predictive ability after leave-one-out cross-validation. Analogous approaches were used for predicting the inhibition of CYP2C9 [64], with data sets (K_i or IC_{50}) ranging in size from 9 to 29. In general, the different Catalyst models included one hydrophobic region and two hydrogen bond acceptor/donor regions. Correlation coefficient between observed and predicted data ranged from 0.71 to 0.91 and allowed to predict the K_i values for 10 to 12/14 compounds of an external set of 14 inhibitors within 1-log unit of observed.

A CoMFA model was developed [65] and refined models were further obtained [66] (q^2 between 0.6 and 0.8) that were able to predict the K_i of an external set of 14 diverse compounds with a mean error of the predictions of 6 μM. A qualitative model, based on alignment-independent GRIND descriptors was developed for discriminating CYP2C9 inhibitors versus non-inhibitors [67]. The PLSD model was based on a data set including 21 inhibitors and 21 non-inhibitors. The model ($r^2 = 0.74$, $q^2 = 0.64$) was externally validated with 14 inhibitors and 25 non-inhibitors: 74% of the entire set was correctly predicted and 13% assigned to a borderline cluster. A quantitative GRIND-based model was also developed using the K_i values of 21 inhibitors. The model ($r^2 = 0.77$, $q^2 = 0.60$) was able to correctly predict 11 out of 12 K_i values within 0.5 log units of observed.

Another approach for modeling CYP2C9 inhibitors applied GRIND descriptors but calculated them from the GRID flexible MIF [68]. In this case, the structures and the K_i of 22

CYP2C9 inhibitors from different chemical classes were used. A model with r^2 of 0.81 and q^2 of 0.62 was obtained, which was able to predict the 11 out of 12 K_i of an external data set within 0.5 log unit. Also in this case, the model developed was in agreement with the information gained from a homology model. Strobl et al. [69] used a CoMFA approach to evaluate the molecular characteristics that are associated with CYP2D6 inhibitory activity. The pharmacophore includes a positive charge on a nitrogen in the middle of a flat hydrophobic region stretching up to 7.5 Å from the nitrogen atom. Other heteroatoms with negative charge and hydrogen bond acceptor properties at the opposite sides of the nitrogen atom show higher inhibitory potency. Ekins et al. [70] developed Catalyst pharmacophores for modeling CYP2D6 competitive inhibitors. These models suggested that the inhibitors are characterized by a hydrogen bond donor and a hydrogen bond acceptor and two to three hydrophobic regions. These models predicted within 1-log unit the K_i of 10 out of 15 compounds considered as external test set. Similar predictability was obtained with a PLS MS-WHIM based QSAR model. For modeling CYP2D6 competitive inhibition, a quantitative GRIND-based model was developed using the K_i values of 47 compounds reported in the literature [71]. The inhibition constants of 17 known drugs and 33 proprietary compounds, representing two independent test sets, were used to validate the model: approximately 74% of the external set was predicted with a K_i error < 1 log unit. Considering a threshold of 5 μM for classifying compounds as strong and weak inhibitors, 78% of the entire external set was correctly predicted, with only 16% false negatives. The model was able to underline the most important features driving CYP2D6 inhibition. In a methodological paper the performance of support vector machine (SVM) in identifying inhibitors of CYP3A4 was evaluated in comparison with PLS-DA [72]. The analysis was performed on IC_{50} data obtained by a radiometric assay using 14C–N-methyl-erythromycin as substrate and recombinant CYP3A4. Compounds were classified as strong ($IC_{50} < 2$ μM), medium or weak (> 20 μM) inhibitors. The overall data set (1345 compounds) was divided into training and a test sets (approximately 60% and 40% of the overall set, respectively). Four different classes of descriptors were used: 2D descriptors calculated with a program developed in house (size, shape, lipophilicity, molar refractivity, atom and ring counts, surface areas, etc.), 2D MOE, Volsurf and a set of 3D descriptors based on semi-empirical AM1 QM calculations. The evaluation indicated that, independently of the descriptors, the models developed using SVM approach were significantly better than those generated using PLS-DA. In particular, using only the simple 2D descriptors a three-class model with 70% accuracy was obtained, suggesting that these techniques are valuable for developing filters for screening virtual libraries.

5.2. Protein-based approaches

As part of work done in the Drug Metabolism Consortium, the combined use of homology modeling and molecular docking was used to define the correct positioning of substrates in CYP2D6 active site. A correlation ($r^2 = 0.61$, $q^2 = 0.59$) was also found between the docking scores calculated with GOLD and the inhibitory characteristics of a series of 33 compounds from the National Cancer Institute database [73]. The method was able to discriminate between tight and weak binding compounds and correctly identified several novel inhibitors.

5.3. Mixed approaches

Also in case of modeling of inhibitors, approaches were proposed in which the structural characteristics of both the inhibitors and proteins were considered. For the identification of CYP2C9 inhibitors, Afzelius et al. [74] used a combined 3D-QSAR and homology approach. The compounds were docked inside the CYP2C9 homology model in order to select the appropriate conformers and alignment to be used in the 3D-QSAR. The data set was divided into a test ($n = 21$) and an external validation set ($n = 8$). The GRID/GOLPE model was able to predict the K_i of the external data set within 0.5 log units of observed. In addition, the interaction energies found relevant in the 3D-QSAR model were in good agreement with the characteristics of the amino acids, which were identified from mutagenesis studies, mainly involved in the recognition of inhibitors.

6. Prediction of inducers

Induction is typically due to activation of ligand-activated transcription factors, which, after further binding with other coactivators, can be transported into the nucleus, where the complex transcriptionally activates the gene. Limited work has been published in this field, as the investigation of the detailed mechanisms of these events and the experimental data started only recently. A couple of comprehensive reviews appeared recently in the literature [75,76].

A number of receptors, which have been shown to regulate CYP transcription, and their associated effects are summarized in Table 5. In many cases, the modeling of ligand–receptor complexes is made difficult by the possibility of a variety of binding modes and orientations and by the simultaneous binding of many small molecules to a single receptor.

Known aryl hydrocarbon receptor (AHR) ligand structures indicate the necessity of planar lipophilic molecules with dimension of 6.8 × 13.7 Å, as concluded by a number of different approaches converged on these conclusions [75,77–79]. A Catalyst pharmacophore model was developed to identify the main structural features of the human Pregnane X receptor (hPXR) ligands. Four hydrophobic and one hydrogen bond acceptor features were required for a good ligand affinity [80].

Table 5
Some receptors and their effects on drug metabolizing enzymes

Receptor	Enzymes regulated
AHR	CYP1A1, CYP1A2, CYP1B1
	GST, UDPGT
PXR	CYP3A, CYP2C8/9, CYP2B6
CAR	CYP2B6, CYP3A4
GR	CYP3A
VDR	CYP3A

Another approach used PLS and Volsurf descriptors for modeling either hPXR or AHR ligands [81]. Pharmacophoric models for constitutive androstane receptors (CAR) pointed out that CAR ligands were characterized by a relatively planar structure with one hydrogen bond acceptor and two or three hydrophobic features in mouse and human, respectively [76]. Another paper dealt with the structural differences between CAR and PXR, based on the available crystallographic data of PXR and vitamin D receptor (VDR). The result of this analysis showed that the size of the ligand cavities in human PXR and CAR are similar but larger than that of VDR. The ability of PXR to accommodate larger ligands was attributed to the flexibility of a surface loop, a feature not present in CAR [82]. An additional QSAR (GOLPE/GRID) model for mouse CAR inhibitors appeared recently in the literature [83]. Catalyst models for glucocorticoid receptor (GR) were also obtained, suggesting that one hydrogen bond donor, a hydrophobic feature and an aromatic hydrophobic region were key for the binding [75].

7. Commercial metabolic reaction databases and expert systems for metabolism prediction

In the previous sections, reference was made to a variety of tools (chemoinformatics, calculation of descriptors, statistical programs, etc.) used for the development of computational models. Some of these are reported in Table 6.

Databases of enzymatic biotransformation reactions and commercially available software for predicting the metabolic fate of xenobiotics [84,85] are summarized in Table 7. In general, these programs cover both phases I and II metabolic pathways of drugs, agrochemicals and industrial chemicals in various species. With the exception of Metasite, these programs are knowledge-based systems, in which the site of metabolism of new chemicals is based on their similarities to known substrates. Knowledge-based systems can be used for discovery and for educational purposes and, in combination with bioanalytical softwares, for proposing hypothesis regarding the structures of potential metabolites, the structure of which may be ambiguously defined by the available bioanalytical methodology.

META is a program developed by Klopman et al. [86,87]. It is an expert system capable, when coupled with appropriate dictionaries of biotransformation pathways, to predict metabolic transformations when molecules are ingested or dumped in the environment.

METEOR is software that predicts the metabolic pathways of xenobiotics from their chemical structure and physicochemical properties [85]. The program contains a knowledge base of structure–metabolism relationships. Each biotransformation describes a metabolic reaction, characteristic of xenobiotics containing a common structural feature. The program also contains generalized rules that take into account the absorption, distribution, and excretion of xenobiotics and their metabolites.

MetabolExpert estimates the structure of metabolites, which might be formed by a substance in humans, animals or in plants. MetabolExpert is a rule-based system with open architecture; in other words, researchers can understand, expand, modify or optimize the data on which the metabolic structural estimation relies.

The MetaSite methodology [34] has been developed to predict the site of metabolism for substrates of 2C9, 2D6, 3A4, 1A2 and 2C19 cytochromes. The site of metabolism can be described by a probability function that is correlated to the free energy of the CYP substrate recognition and reactivity process. MetaSite uses GRID-based representations of the CYP enzymes, which are pre-computed and stored in the software.

Table 6
Some general commercial software for predicting the metabolism endpoints mentioned in this review

Company	Product	URL
Accelrys	Cerius2, Catalyst, QUANTA Discovery Studio, Pipeline Pilot	www.accelrys.com
Biorad	KnowItAll	http://www.bio-rad.com/
Cambridge Crystallographic Data Center	GOLD	http://www.ccdc.cam.ac.uk/
Frankfurt University	CATS light	http://gecco.org.chemie.uni-frankfurt.de/gecco.html
Golden Helix	Chemtree	http://www.goldenhelix.com/index.jsp
Inpharmatica	ADMENSA	http://www.inpharmatica.co.uk/
MIA	GOLPE, Almond	http://www.miasrl.com/
Milano Chemometrics and QSAR Research Group	Dragon (includes WHIM)	http://www.talete.mi.it/dragon.htm
Molecular Discovery	GRID, Volsurf, Almond (GRIND)	www.moldiscovery.com
Schrödinger	Qikprop	http://www.schrodinger.com
Tripos	Sybyl, Volsurf, Almond, BCUT	http://www.tripos.com/
UCSF	DOCK	http://dock.compbio.ucsf.edu/

Table 7
Some tools and rule-based systems for the prediction of metabolites

Company	Product	URL
Accelrys	Biotransformation database	www.accelrys.com
Compudrug	MetabolExpert, MEXAlert	www.compudrug.com
Lhasa	METEOR	http://www.chem.leeds.ac.uk/LUK/
MDL information system	Metabolite database	www.mdl.com
Molecular Discovery	Metasite	www.moldiscovery.com
Multicase	METAPC	www.multicase.com

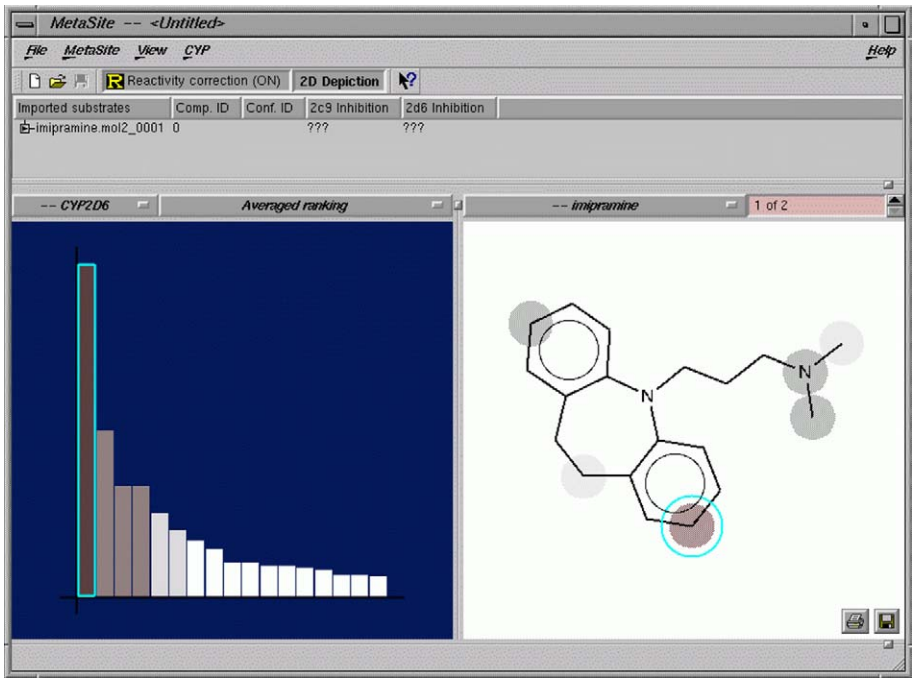

Fig. 3. Snapshot of a typical output of MetaSite software. Imipramine has been shown as example. The heteroatoms and the corresponding hydrogen atoms in the molecule that are predicted as the most probable metabolic sites are highlighted in brown and dark-gray colors. The same results are provided graphically (i.e. the highest-brown bars represent the most probable site/s of metabolism) on the left hand part of the window.

Conversely, semi-empirical QM calculations for charges and reactivity are automatically performed only on substrate molecules. An example of the output provided by MetaSite software is reported in Fig. 3.

8. Conclusions and future perspectives

In the last few years, pharmaceutical companies made big investments for setting up early experimental screens to evaluate metabolic endpoints, due to the recognition that metabolism properties leading to important drug–drug interactions are one of the most important reasons for failure of new drugs. The subsequent availability of large databases of metabolic properties of compounds prompted the efforts in developing structure-based computational tools that may be used at lower cost and even before the actual drug candidate is synthesized. Functional to this was also the increased number of the alternative computational approaches and the availability of critical biological and mechanistic information on drug metabolizing enzymes activity and regulation. Of particular relevance in this field was the resolution of the crystal structure of some drug metabolizing enzymes [9–13].

Although we are facing an unprecedented blossoming of new computational models for predicting metabolic endpoints, there is still much to do, to increase the confidence in the in silico models [88]. In some cases the computational models reported in the literature are sub optimal as they are derived from small data sets. Also, the experimental measurements are affected by high variability or their relevance with respect to the in vivo situation is not fully exploited. Naturally, this should be put into the context of the drug discovery process. The questions that must be answered are different depending on the phases of the drug development continuum. In general, the answers must be more and more refined as long as new information is obtained. In the very early phases, “global” and fast approaches should be used as rough filters on large libraries of compounds. In this respect, tools showing even a small gain compared to a random choice may suffice to enrich libraries with “druggable” compounds. Later on, when experimental data are of better quality, models developed on more focused series of compounds should give more precise and accurate predictions.

Other issues in the scientific literature covering this field are related to the relative paucity of information. In many cases due to intellectual property or practical issues the data sets on which these models are developed remain undisclosed. In the same way, and possibly for the same reasons, the description of the parameterization of the models is sometime inadequate to verify the applicability of the models to new data sets. In this respect, more transparency is needed to make these approaches publicly available. In some cases, the validation of the model is not always of adequate quality. In other cases, the strategy of implementation and the utility of the model in the drug discovery process is not fully disclosed. This is an issue of particular importance, because to create confidence in these tools, it must be absolutely avoided the impression of performing sophisticated but sterile computational exercises, with minimal impact on the drug development business. Analogous problems are present in commercial models. In many cases, the use of these models as black boxes prevents the achievement of satisfactory predictions. In our group we tested some global models related to metabolic stability and CYP inhibition. The absence of

knowledge of the training set on which the models were developed biased the evaluation of compounds from the literature and, in many cases, when tested with proprietary compounds the accuracy of the models was substantially poor. On the contrary, the tools aiming to the prediction of the site of metabolism, gave predictions of good quality (typically in 80% of cases, the observed major pathway was predicted within the first two or three most probable ones).

A specific item that possibly deserves more attention is the prediction of rates of metabolism. It may be that the scarcity of data, the complexity of this phenomenon and its dependence on numerous factors are limiting the availability of approaches aiming to the prediction of this property. The adoption of mixed or consensus approaches in this field, as well as for the prediction of other properties, may improve the situation. The consensus approaches to improve either the sensitivity or the selectivity of models is becoming more popular. The integration of information derived from different sources should be pursued, possibly adopting meta-models to make the most efficient use of the information derived from in silico, in vitro and in vivo approaches.

In conclusion, the application of in silico tools in the prediction of metabolic endpoints is in its first phase and many questions regarding these applications will likely be answered in the next few years.

References

[1] F. Lombardo, E. Gifford, M.Y. Shalaeva, Mini Rev. Med. Chem. 3 (2003) 861–875.
[2] H. van der Waterbeemd, E. Gifford, Nat. Rev. Drug Discov. 2 (2003) 192–204.
[3] A. Boobis, U. Gundert-Remy, P. Kremers, P. Macheras, O. Pelkonen, Eur. J. Pharm. Sci. 17 (2002) 183–193.
[4] A.G.E. Wilson, A.C. White, R.A. Mueller, Curr. Opin. Drug Discov. Dev. 6 (2003) 123–128.
[5] A.P. Beresford, M. Segall, M.H. Tarbit, Curr. Opin. Drug Discov. Dev. 7 (2004) 36–42.
[6] D.F.V. Lewis, Xenobiotica 28 (1998) 617.
[7] M. Bertrand, P. Jackson, P. Walther, Eur. J. Pharm. Sci. 11 (2 Suppl.) (2000) S61–S72.
[8] I. Schlichting, J. Berendze, K. Chu, A.M. Stoch, S.A. Maves, D.E. Benson, R.M. Sweet, D. Ringe, G.A. Petsko, S.G. Sligar, Science 287 (2000) 1615–1622.
[9] P.A. Williams, J. Cosme, V. Sridhar, E.F. Johnson, D.E. McRee, Mol. Cell 5 (2000) 121–131.
[10] P.A. Williams, J. Cosme, A. Ward, H.C. Angove, D.M. Vinkovic, H. Jhoti, Nature 424 (2003) 464–468.
[11] P.A. Williams, J. Cosme, D.M. Vinkovic, A. Ward, H.C. Angove, P.J. Day, C. Vonrhein, I.J. Tickle, H. Jhoti, Science 305 (2004) 683–686.
[12] M.R. Wester, J.K. Yano, G.A. Schoch, C. Yang, K.J. Griffin, C.D. Stout, E.F. Johnson, J. Biol. Chem. 279 (2004) 35630–35637.
[13] J.K. Yano, M.R. Wester, G.A. Schoch, K.J. Griffin, C.D. Stout, E.F. Johnson, J. Biol. Chem. 279 (2004) 38091–38094.
[14] C. de Graaf, N.P.E. Vermeulen, A. Feenstra, J. Med. Chem. 48 (2005) 2725–2755.
[15] D.A. Smith, B.C. Jones, D.K. Walker, Med. Res. Rev. 16 (1996) 243–266.
[16] A.-E.F. Nassar, P.E. Adams, Curr. Drug Metab. 4 (2003) 259–271.
[17] K.R. Korzekwa, J. Grogan, S. DeVito, J.P. Jones, in: R.R. Snyder, J.J. Kocsis, I.G. Sipes, G.F. Kalf, D.J. Jollow, H. Greim, T.J. Monks, C.M. Witmer (Eds.), Advances in Experimental Medicine and Biology V, Springer-Verlag, Berlin, 1996, pp. 361–369 (387 pp).
[18] K.R. Korzekwa, J.P. Jones, J.R. Gillette, J. Am. Chem. Soc. 112 (1990) 7042–7046.
[19] J.P. Jones, M. Mysinger, K.R. Korzekwa, Drug Metab. Dispos. 30 (2002) 7–12.
[20] S.B. Singh, L.Q. Shen, M.J. Walker, R.P. Sheridan, J. Med. Chem. 46 (2003) 1330–1336.
[21] L. Koymans, N.P.E. Vermeulen, S.A. van Acker, J.M. Koppele, J.J. Heykants, K. Lavrijsen, W. Meuldermans, G.M. Donne-Op den Kelder, Chem. Res. Toxicol. 5 (1992) 211–219.
[22] D.F.V. Lewis, B.G. Lake, Xenobiotica 26 (1996) 723–753.
[23] D.F.V. Lewis, P.J. Eddershaw, P.S. Goldfarb, M.H. Tarbit, Xenobiotica 26 (1996) 1067–1086.
[24] D.F.V. Lewis, P.J. Eddershaw, P.S. Goldfarb, M.H. Tarbit, Xenobiotica 27 (1997) 319–339.
[25] M.J. de Groot, N.P.E. Vermeulen, J.D. Kramer, F.A.A. van Acker, G.M. Donne-Op den Kelder, Chem. Res. Toxicol. 9 (1996) 1079–1091.
[26] S. Modi, M.J. Paine, M.J. Sutcliffe, L.-Y. Lian, W.U. Primrose, C.R. Wolf, G.C,K. Roberts, Biochemistry 35 (1996) 4540–4550.
[27] V.A. Payne, Y.-T. Chang, G.H. Loew, Proteins 37 (1999) 176–190.
[28] D.F.V. Lewis, M.G. Bird, M. Dickins, B.G. Lake, P.J. Eddershaw, M.H. Tarbit, P.S. Goldfarb, Xenobiotica 30 (2000) 1–25.
[29] D.F.V. Lewis, Drug Metab. Rev. 34 (2002) 55–67.
[30] D.F.V. Lewis, B.G. Lake, M. Dickins, P.S. Goldfarb, Xenobiotica 34 (2004) 549–569.
[31] M.J. de Groot, M.J. Ackland, V.A. Horne, A.A. Alex, B.C. Jones, J. Med. Chem. 42 (1999) 1515–1524.
[32] M.J. de Groot, M.J. Ackland, V.A. Horne, A.A. Alex, B.C. Jones, J. Med. Chem. 42 (1999) 4062–4070.
[33] M.J. de Groot, A.A. Alex, B.C. Jones, J. Med. Chem. 45 (2002) 1983–1993.
[34] I. Zamora, L. Afzelius, G. Cruciani, J. Med. Chem. 46 (2003) 2313–2324.
[35] M. Ingelman-Sundberg, Pharmacogenom. J. 5 (2005) 6–13.
[36] S. Ekins, G. Bravi, J.H. Wikel, S.A. Wrighton, J. Pharmacol. Exp. Ther. 291 (1999) 424–433.
[37] S. Ekins, G. Bravi, B.J. Ring, T.A. Gillespie, J.S. Gillespie, M. Vandenbranden, S.A. Wrighton, J.H. Wikel, J. Pharmacol. Exp. Ther. 288 (1999) 21–29.
[38] D.F.V. Lewis, S. Modi, M. Dickins, Drug Metab. Rev. 34 (2002) 69–82.
[39] S. Haji-Momenian, J.M. Rieger, T.L. Macdonald, M.L. Brown, Bioorg. Med. Chem. 11 (2003) 5545–5554.
[40] D. Korolev, K.V. Balakin, Y. Nikolsky, E. Kirillov, Y.A. Ivanenkov, N.P. Savchuk, A.A. Ivashchenko, T. Nikolskaya, J. Med. Chem. 46 (2003) 3631–3643.
[41] K.V. Balakin, S. Ekins, A. Bugrim, Y.A. Ivanenkov, D. Korolev, Y.V. Nikolsky, A.V. Skorenko, A.A. Ivashchenko, N.P. Savchuk, T. Nikolskaya, Drug Metab. Dispos. 32 (2004) 1183–1189.
[42] Q. Wang, J.R. Halpert, Drug Metab. Dispos. 30 (2002) 86–95.
[43] F. De Rienzo, F. Fanelli, M.C. Menziani, P.G. De Benedetti, J. Comput. Aided Mol. Des. 14 (2000) 93–116.
[44] R. Snyder, R. Sangar, J. Wang, S. Ekins, Quant. Struct.-, Act. Relat. 21 (2002) 357–368.
[45] S. Ekins, R.S. Obach, J. Pharmacol. Exp. Ther. 295 (2000) 463–473.
[46] M. Shen, Y. Xiao, A. Golbraikh, V.K. Gombar, A. Tropsha, J. Med. Chem. 46 (2003) 3013–3020.
[47] B.F. Jensen, M.D. Sorensen, A.-M. Kissmeyer, F. Bjoerkling, K. Sonne, S.B. Engelsen, L. Norgaard, J. Comput. Aided Mol. Des. 17 (2004) 849–859.
[48] P. Crivori, I. Zamora, B. Speed, C. Orrenius, I. Poggesi, J. Comput. Aided Mol. Des. 18 (2004) 55–66.
[49] K.V. Balakin, S. Ekins, A. Bugrim, Y.A. Ivanenkov, D. Korolev, Y.V. Nikolsky, A.A. Ivashchenko, N.P. Savchuk, T. Nikolskaya, Drug Metab. Dispos. 32 (2004) 1111–1120.
[50] S. Bellosta, R. Paoletti, A. Corsini, Circulation 109 (23 Suppl. 1) (2004) III50–III57.
[51] S. Boyer, I. Zamora, J. Comput. Aided Mol. Des. 16 (2002) 403–413.
[52] R.G. Susnow, S.L. Dixon, J. Chem. Inf. Comput. Sci. 43 (2003) 1308–1315.
[53] S. Ekins, J. Berbaum, Drug Metab. Dispos. 31 (2003) 1077–1080.

[54] J. Zuegge, U. Fechnera, O. Roche, N.J. Parrott, O. Engkvist, G. Schneider, Quant. Struct.-, Act. Relat. 21 (2002) 249–256.
[55] L. Molnar, G.M. Keserü, Bioorg. Med. Chem. Lett. 12 (2002) 419–421.
[56] T. Moon, M. Hwan Chi, D.-H. Kim, C.N. Yoon, Y.S. Choi, Quant. Struct.-, Act. Relat. 19 (2000) 257–263.
[57] S.E. O'Brien, M.J. de Groot, J. Med. Chem. 48 (2005) 1287–1291.
[58] A.C. White, R.A. Mueller, R.H. Gallavan, S. Aaron, A.G.E. Wilson, Mutat. Res. 539 (2003) 77–89.
[59] P.R. Ortiz de Montellano, M.A. Correia, in: P.R. Ortiz de Montellano (Ed.), Cytochrome P450: Structure Mechanism and Biochemistry, second ed, Plenum Press, New York, 1995, pp. 305–364.
[60] A. Poso, J. Gynther, R. Juvonen, J. Comput. Aided Mol. Des. 15 (2001) 195–202.
[61] A. Asikainen, J. Tarhanen, A. Poso, M. Pasanen, E. Alhava, R.O. Juvonen, Toxicol. In Vitro 17 (2003) 449–455.
[62] M. Rahnasto, H. Raunio, A. Poso, C. Wittekindt, R.O. Juvonen, J. Med. Chem. 48 (2005) 440–449.
[63] S. Ekins, G. Bravi, S. Binkley, J.S. Gillespie, B.J. Ring, J.H. Wikel, S.H. Wrighton, J. Pharmacol. Exp. Ther. 290 (1999) 429–438.
[64] S. Ekins, G. Bravi, S. Binkley, J.S. Gillespie, B.J. Ring, J.H. Wikel, S.A. Wrighton, Drug Metab. Dispos. 28 (2000) 994–1002.
[65] J.P. Jones, M.X. He, W.F. Trager, A.E. Rettie, Drug Metab. Dispos. 3 (1996) 1–18.
[66] S. Rao, R. Aoyama, M. Schrag, W.F. Trager, A. Rettie, J.P. Jones, J. Med. Chem. 43 (2000) 2789–2796.
[67] L. Afzelius, C.M. Masimirembwa, A. Karlen, T.B. Andersson, I. Zamora, J. Comput. Aided Mol. Des. 16 (2002) 443–458.
[68] L. Afzelius, I. Zamora, C.M. Masimirembwa, A. Karlen, T.B. Andersson, S. Mecucci, M. Baroni, G. Cruciani, J. Med. Chem. 47 (2004) 907–914.
[69] G.R. Strobl, S. von Kruedener, J. Stockigt, F.P. Guengerich, T. Wolff, J. Med. Chem. 36 (1993) 1136–1145.
[70] S. Ekins, G. Bravi, S. Binkley, J.S. Gillespie, J.B.J. Ring, J.H. Wikel, S.A. Wrighton, Pharmacogenetics 9 (1999) 4774–4789.
[71] P. Crivori, I. Poggesi, Basic Clin, Pharmacol. Toxicol. 96 (2005) 251–253.
[72] J.M. Kriegl, T. Arnhold, B. Beck, T.A. Fox, J. Comput. Aided Mol. Des. 19 (2005) 189–201.
[73] C.A. Kemp, J.U. Flanagan, A.J. van Eldik, J.D. Marechal, C.R. Wolf, G.C. Roberts, M.J. Paine, M.J. Sutcliffe, J. Med. Chem. 47 (2004) 5340–5346.
[74] L. Afzelius, I. Zamora, M. Ridderstrom, T.B. Andersson, A. Karlen, C.M. Masimirembwa, Mol. Pharmacol. 59 (2001) 909–919.
[75] D.C. Mankowski, S. Ekins, Curr. Drug Metab. 4 (2003) 381–391.
[76] S. Ekins, L. Mirny, E.G. Schuetz, Pharm. Res. 19 (2002) 1788–1800.
[77] D.F.V. Lewis, M.N. Jacobs, M. Dickins, B.G. Lake, Toxicol. 176 (2002) 51–57.
[78] A. Vedani, M. Dobler, J. Med. Chem. 45 (2002) 2139–2149.
[79] M. Procopio, A. Lahm, A. Tramontano, D. Pitea, Eur. J. Biochem. 269 (2002) 13–18.
[80] S. Ekins, J.A. Erikson, Drug Metab. Disp. 30 (2002) 96–99.
[81] M.N. Jacobs, Toxicology 205 (2004) 43–53.
[82] L. Xiao, X. Cui, V. Madison, R.E. White, K.C. Cheng, Drug Metab. Disp. 30 (2002) 951–956.
[83] J. Jyrkkää, J. Mäkinen, J. Gynther, H. Savolainen, A. Poso, P. Honkakoski, J. Med. Chem. 46 (2003) 4687–4695.
[84] J. Langowski, A. Long, Adv. Drug Deliv. Rev. 31 (2002) 407–415.
[85] B. Testa, A.-L. Balmat, A. Long, Pure Appl. Chem. 76 (2004) 907–914.
[86] G. Klopman, M. Dimayuga, J. Talafous, J. Chem. Inf. Comput. Sci. 34 (1994) 1320–1325.
[87] J. Talafous, L.M. Sayre, J.J. Mieyal, G. Klopman, J. Chem. Inf. Comput. Sci. 34 (1994) 1326–1333.
[88] T.R. Stouch, J.R. Kenyon, S.R. Johnson, X.Q. Chen, A. Doweyko, Y. Li, J. Comput. Aided Mol. Des. 17 (2003) 83–92.